CERN LIBRARIES, GENEVA

CM-P00064589

LEP Commissioning Note 17

Coupling in LEP: Characteristics of the source (I)

9 November 1989

CERNVM/FAUCHET

COUPLING.tex

A.M. Fauchet, J.P. Gourber, J.P. Koutchouk, T. Risselada

Keywords: OPTICS

No run numbers specified.

Summary

This note summarizes the results of an early experiment (August) designed to investigate the source of coupling in the LEP machine. Coupling is quantified by the horizontal to vertical orbit transfer.

The most important results are that the source is distributed in the LEP arcs only. It essentially scales with 1/Energy, indicating an energy independent magnetic field source. Its harmonic content is such that the initial choice of tune split ($Q_x - Q_y \approx 8$)had to be changed to minimize the excitation of the linear coupling resonance.

Contents

1 Aims and Methodology 1

2 Analysis of the Data 2

2.1 Horizontal bumps in the arcs 2
2.2 Horizontal bumps in the straight sections 4
2.3 Harmonic analysis of the coupling source 4
2.4 Distribution of the coupling source within the arcs 4
2.5 Symmetry of the coupling source 5
2.6 Linearity of coupling 5
2.7 Contribution of the orbit displacement in the sextupoles 5

3 Conclusion 5

4 Acknowlegments 6

1 Aims and Methodology

Early during LEP start-up it became apparent that a large coupling existed in the machine with the nominal optics B80A20 ($Q_x = 70.44, Q_y = 78.37$), in the absence of any of

the experimental solenoids and compensating skew quadrupoles. Although localized coupling sources were initially suspected, analysis of the transfer of the horizontal injection oscillations to the vertical plane ruled out this hypothesis [1].

The measurements reported here were planned to investigate the characteristics of the coupling in order to understand its source and compensate it.

The principle of the measurement is to excite an oscillation of the horizontal orbit in a limited section of the machine and measure the resulting perturbation of the vertical orbit.

The following properties of the coupling source were investigated:

- Location of the coupling source: it was tested with closed horizontal bumps in each arc and two straight sections.
- Symmetry of the coupling source, namely whether the source is a skew quadrupole or a skew sextupole.
- Linearity of the coupling: The horizontal to vertical orbit transfer was measured as a function of the amplitude of the horizontal bump.
- Energy dependence: Measurements of the horizontal to vertical orbit transfer were done at injection energy (20 GeV) and flat-top energy (approximately 45 GeV).

The measurements were done on Monday, August 21, Wednesday the 23rd and Sunday the 27th. Orbits were stored in directories mrx/monday21, mrx/wednesday23, mrx/sunday27. The LEP optics were B80B20 ($Q_x \sim 71.38, Q_y \sim 78.28$) with experimental solenoids and skew quadrupoles off, a single beam and separators off.

2 Analysis of the Data

2.1 Horizontal bumps in the arcs

Closed horizontal bumps covering successively each whole arc were introduced and the resulting vertical orbit distortion measured. Given the good initial closed orbit, the horizontal amplitude could reach 25 mm at the PUs, i.e. 43 mm at β_{max}. Bumps of the same strength were used in each arc. Data was taken at 20 GeV (Monday, 21st and Sunday, 27th) and at approximately 45 GeV (Wednesday, 23rd). In order to improve the accuracy and eliminate systematic errors, differences were taken between orbits with horizontal bumps of opposite signs. Figure 1 shows such an orbit difference for a closed horizontal bump in arc 8.

The overall results of the measurements in the arcs are shown on figure 2, which displays a plot of the vertical rms σ_y (calculated over all PUs, after elimination of the bad PUs) of the difference orbits versus the position of the horizontal bump (arc number). To overcome any calibration problem, the data have been normalized to a ± 17 mm amplitude for the horizontal bump on the difference orbit.

Figure 2 shows that the coupling can be separated into an arc independent part, plus a weaker component with periodicity 1 around the LEP ring. It is thus possible that there

are two or more superimposed coupling sources. The difference between the two 20 GeV curves gives us an estimate of the uncertainty on the data.

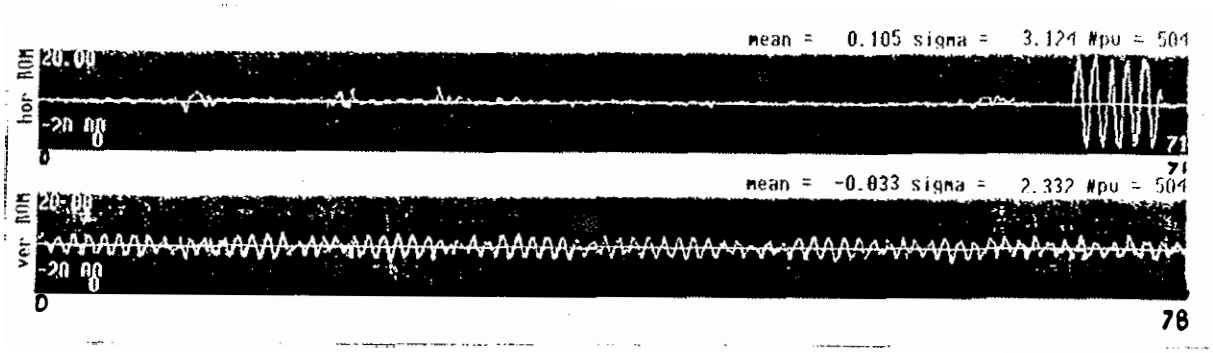

Figure 1: Effect of a closed horizontal bump in Arc 8

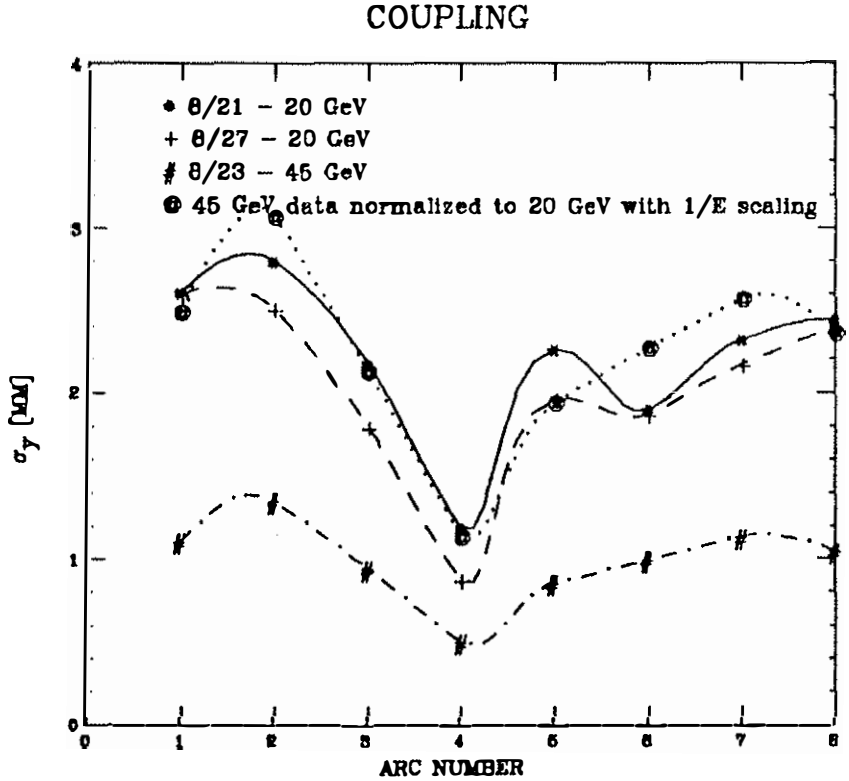

Figure 2: Vertical orbit distortion σ_y vs. location of the horizontal bump

In order to assess the energy dependence, the 45 GeV data has been scaled down to 20 GeV using a 1/Energy law, which is the dotted curve on Figure 2. It can be seen from the figure that within the error bars all sources of coupling give an effect which scales

with inverse energy. We therefore expect the source to be a constant skew quadrupole or sextupole.

2.2 Horizontal bumps in the straight sections

Horizontal bumps were introduced in interaction points 2 and 6 (IP2 and IP6). No vertical orbit change could be detected as a result of the horizontal bump. Therefore the coupling source is not located in the straight sections.

2.3 Harmonic analysis of the coupling source

Harmonic analysis of the data shown on figure 2 yields the spectrum shown on figure 3. The dominant contribution is the dc component, which produces strong coupling for a tune split of $Q_x - Q_y \approx 0 + 8k$. This mixing is due to the modulation effect of the straight sections. Although weaker, the first harmonic is still significant (probably related to the earth magnetic field). Taking into account the modulation by the straight sections, the tune splits which minimizes betatron coupling are 6 or 10 (2 ± 8).

```
ORBCOR  -  harmonic coefficients and phases

 nr    strength      phase

  0      2.3939      0.0000   ****************************************
  1      0.6727      0.0160   ************
  2      0.3357      0.0885   *****
  3      0.3444      0.0680   *****
  4      0.2768      0.0585   ****
```

Figure 3: Harmonic analysis of the coupling source

2.4 Distribution of the coupling source within the arcs

A more detailed analysis of the vertical orbit distortion than the simple computation of σ_y can give a picture of the parasitic field inside the arc.

Method: If the beam was injected on the closed orbit, one would see no oscillation transfer until the horizontal bump, and then a growth of the vertical oscillation within the bump, dependent on the distribution of the coupling source. The drawback of this method is the lower accuracy of the PU's in single turn mode. It can however be simulated with the collected closed orbit data: a betatronic oscillation is fitted to the measured vertical closed orbit upstream of the horizontal bump. It is then subtracted from the measured vertical orbit all around the ring. The resulting orbit is similar to a single turn trajectory. Figures 5 and following show the the reconstructed vertical trajectory at 20 GeV in each arc and in addition at 46 GeV in arc 4.

Results: With the exception of arcs 3 and 4, the arcs are essentially identical and show a regular increase of the trajectory amplitude from the beginning to the end of the bump,

which does indicate a uniform distribution of the parasitic fields. Arc 3 shows a smaller amplitude for the vertical trajectory but the amplitude still seems to increase along the length of the arc as in the other arcs. On the other end, arc 4 shows a small oscillation of constant amplitude, and little or no increase in amplitude along the arc at 20 GeV or at 46 GeV. Furthermore, since for arc 4 the amplitude of the vertical oscillation is comparable to the error bars on the data, the vertical oscillation amplitude might even be smaller than 20% of the amplitude in the other arcs.

2.5 Symmetry of the coupling source

The goal was to determine whether the coupling source had the symmetry of a skew quadrupole or a skew sextupole. The experiment was carried out only in arc 2. A special closed bump, made of a sequence of identical π bumps was applied first towards positive x's then towards negative x's. For both cases the transfer of orbit distorsion from the horizontal to the vertical plane was measured. Normalized to π bumps of equal amplitudes, the vertical orbit oscillation has σ_y of 0.464 mm for the positive bumps and 0.421 mm for the negative bumps. The difference being about 10%, it appears that the coupling coefficient is essentially a skew quadrupole component.

2.6 Linearity of coupling

Figure 4 shows that the peak-to-peak vertical orbit distortion induced by a closed bump in arc 2 is linear with the amplitude of this bump. This is consistent with little or no skew sextupole component as discussed in the previous paragraph. The scaling of the vertical oscillations amplitude to the same horizontal bump amplitude, as done in Figure 2, is thus legitimate.

2.7 Contribution of the orbit displacement in the sextupoles

Although the betatron coupling is far above what could be expected from imperfect vertical orbit in sextupoles, a quick check was done by increasing by 5 units the chromaticities and measuring again arc 6. The rms σ_y of the vertical oscillation induced by a closed horizontal bump was 1.90 mm, to be compared to 1.82 mm for nominal chromaticity. Thus within the limited accuracy of the measurement, sextupoles do not create unexpected problems.

3 Conclusion

- The coupling source is distributed in the arcs and not in the straight-sections.
- The coupling is linear to a good accuracy, and essentially all due to a skew quadrupole component.
- All arcs have a coupling source of comparable strength, uniformely distributed along the arc, except for arcs 3 and 4. Arc 3 also shows a coupling source uniformely

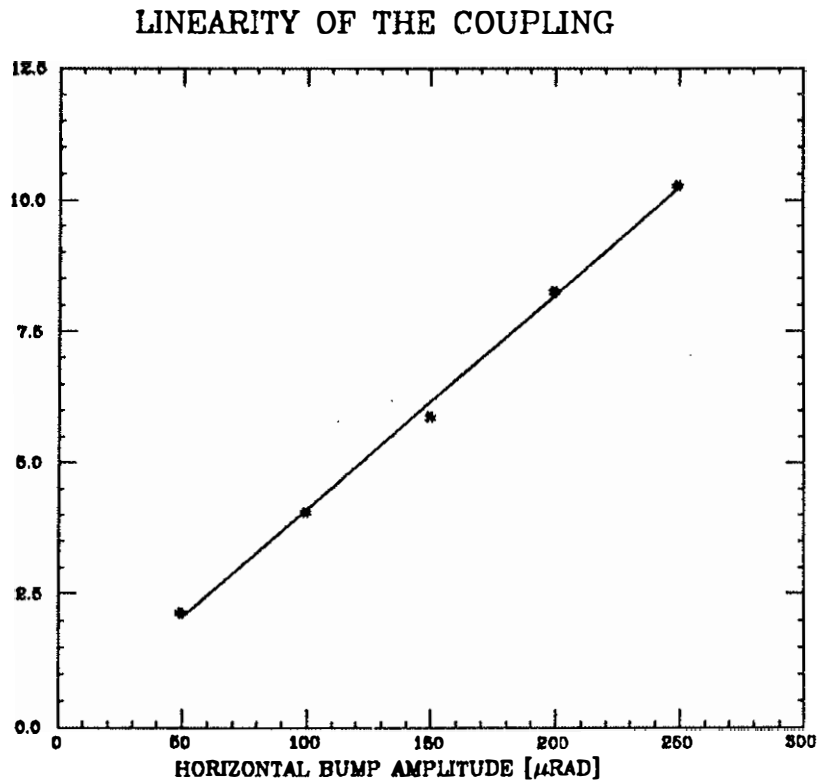

Figure 4: σ_y vs. horizontal bump amplitude

distributed along the arc, but of reduced strength. As for arc 4, the coupling source seems localized at the beginning of the arc and of much reduced strength.

- The fundamental and first harmonic of the spectrum of the coupling source should be avoided. A tune split of 6, which makes the machine sensitive to the harmonic 2 of the coupling sources, seems optimal.
- The source seems an energy independent magnetic field to the accuracy of the measurements done.

4 Acknowlegments

The authors would like to acknowledge the contribution of many people, in particular A. Millich, T. Fieguth, F. Ruggiero and E. Weihreter who participated in the shifts, both for the data presented here and earlier shifts dedicated to understanding the coupling.

References

[1] Optics Commissioning Team, LEP log book.

it 2 ** LEP ring - measured orbit + β oscillation
VERT plane

monitor	y (mm)
PU.QL18.R1	1.32
PU.QL28.R1	-0.71
PU.QL4.R1	-2.35
PU.QL5.R1	0.29
PU.QL6.R1	-0.28
PU.QL7.R1	-0.29
PU.QL8.R1	-1.22
PU.QL9.R1	-0.21
PU.QL10.R1	0.88
PU.QL11.R1	0.29
PU.QL12.R1	0.70
PU.QL14.R1	-0.25
PU.QL15.R1	-0.35
PU.QL16.R1	-0.27
PU.QL17.R1	-0.08
PU.QL18.R1	-0.32
PU.QD20.R1	1.25
PU.QD22.R1	0.93
PU.QD24.R1	1.15
PU.QD26.R1	0.18
PU.QD28.R1	-3.13
PU.QD30.R1	
PU.QD32.R1	0.11
PU.QD34.R1	1.48
PU.QD36.R1	1.52
PU.QD38.R1	0.94
PU.QD40.R1	-4.07
PU.QD42.R1	-2.13
PU.QD44.R1	0.18
PU.QD46.R1	0.92
PU.QD48.R1	3.30
PU.QD48.L2	0.53
PU.QD46.L2	-2.04
PU.QD44.L2	-3.53
PU.QD42.L2	0.82
PU.QD40.L2	2.83
PU.QD38.L2	4.68
PU.QD36.L2	1.30
PU.QD34.L2	-2.59
PU.QD32.L2	-5.04
PU.QD30.L2	-0.13
PU.QD28.L2	3.82
PU.QD26.L2	6.35
PU.QD24.L2	3.70
PU.QD22.L2	-2.89
PU.QD20.L2	-6.42
PU.QS18.L2	-2.19
PU.QS17.L2	0.22
PU.QS16.L2	3.15
PU.QS15.L2	2.65
PU.QS14.L2	5.44
PU.QS12.L2	-1.21

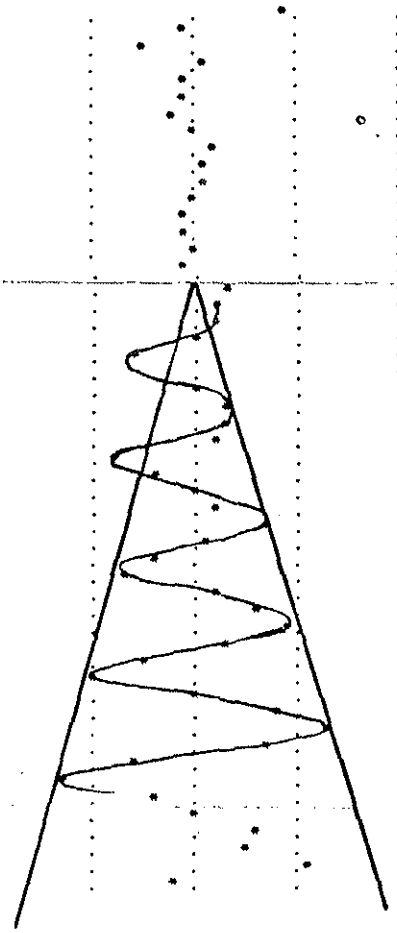

ARC 1-2
20 GeV

Figure 5

it 3 ** LEP ring - measured orbit + β oscillation
VERT plane

monitor	y (mm)
PU.QS0.R2	
PU.QS1A.R2	0.37
PU.QS2A.R2	0.29
PU.QS4.R2	0.28
PU.QS5.R2	0.04
PU.QS6.R2	0.16
PU.QS7.R2	-0.11
PU.QS8.R2	-0.06
PU.QS9.R2	0.30
PU.QS10.R2	0.08
PU.QS11.R2	0.06
PU.QS12.R2	-0.08
PU.QS14.R2	0.13
PU.QS15.R2	0.78
PU.QS16.R2	0.57
PU.QS17.R2	0.57
PU.QS18.R2	0.05
PU.QD20.R2	-0.43
PU.QD22.R2	4.30
PU.QD24.R2	0.90
PU.QD26.R2	1.37
PU.QD28.R2	
PU.QD30.R2	-1.19
PU.QD32.R2	-1.93
PU.QD34.R2	2.04
PU.QD36.R2	1.41
PU.QD38.R2	0.95
PU.QD40.R2	-0.50
PU.QD42.R2	-2.73
PU.QD44.R2	-1.09
PU.QD46.R2	-1.23
PU.QD48.R2	3.40
PU.QD48.L3	3.16
PU.QD46.L3	-1.93
PU.QD44.L3	-4.01
PU.QD42.L3	-2.11
PU.QD40.L3	1.76
PU.QD38.L3	4.99
PU.QD36.L3	4.82
PU.QD34.L3	-2.42
PU.QD32.L3	-5.26
PU.QD30.L3	-2.74
PU.QD28.L3	1.58
PU.QD26.L3	6.90
PU.QD24.L3	5.11
PU.QD22.L3	-1.88
PU.QD20.L3	-6.90
PU.QL18.L3	-4.94
PU.QL17.L3	-0.57
PU.QL16.L3	2.33
PU.QL15.L3	3.05
PU.QL14.L3	6.15

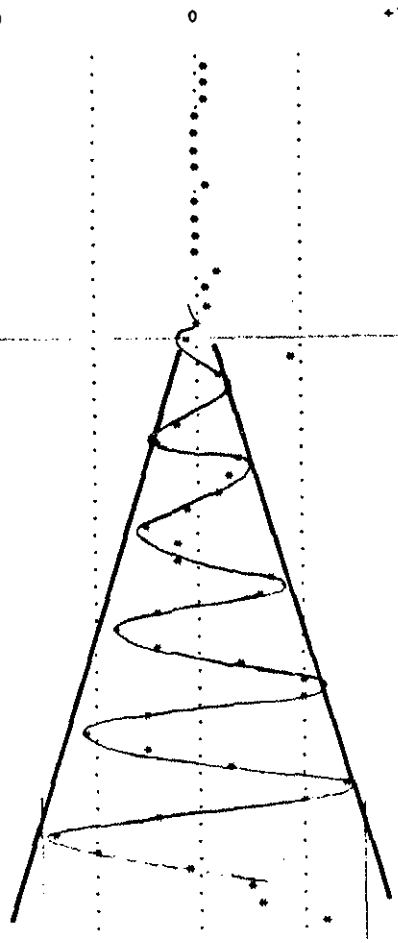

ARC 2-3
20 GeV

Figure 6

it 2 ** LEP ring - measured orbit + β oscillation
VERT plane

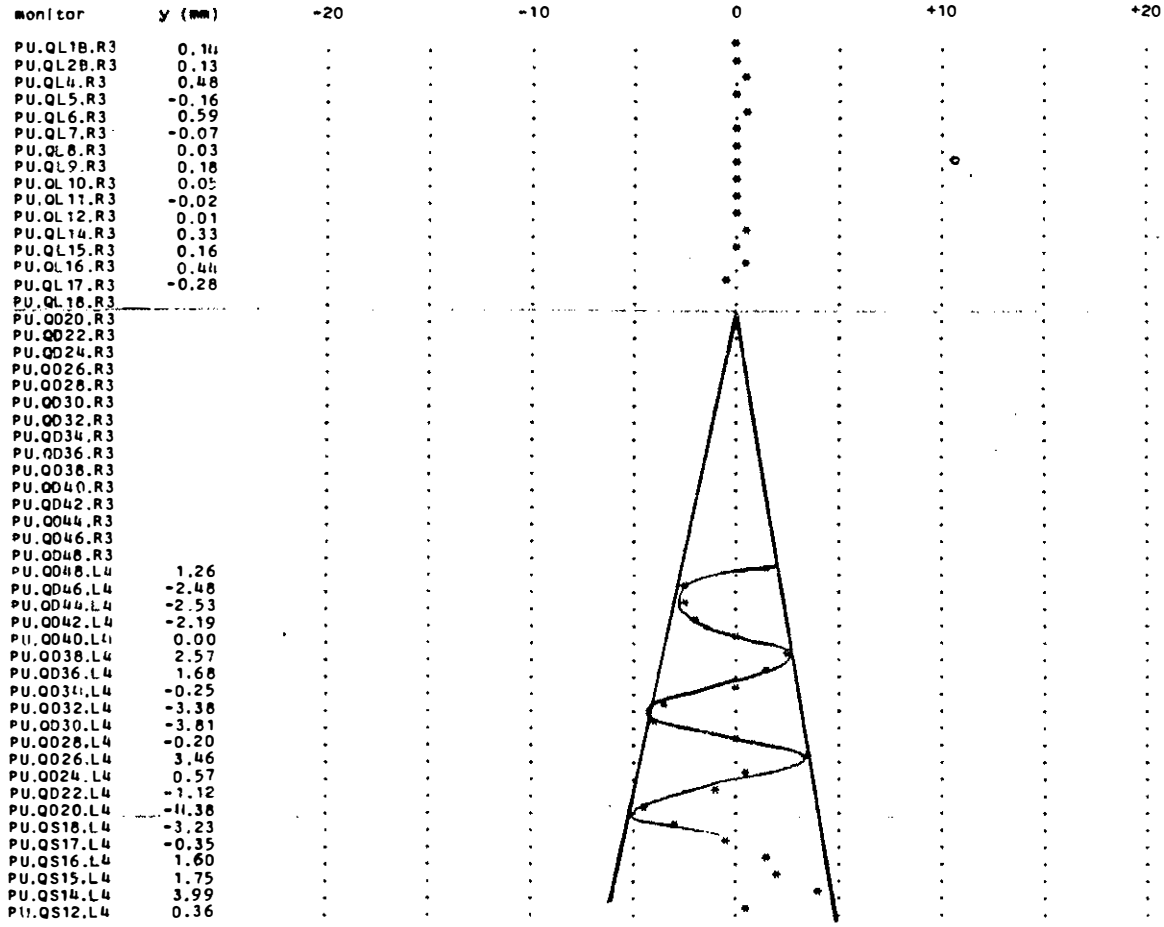

ARC 3-4
20 GeV

beam

Figure 7

it 2 ** LEP ring - measured orbit + β oscillation
VERT plane

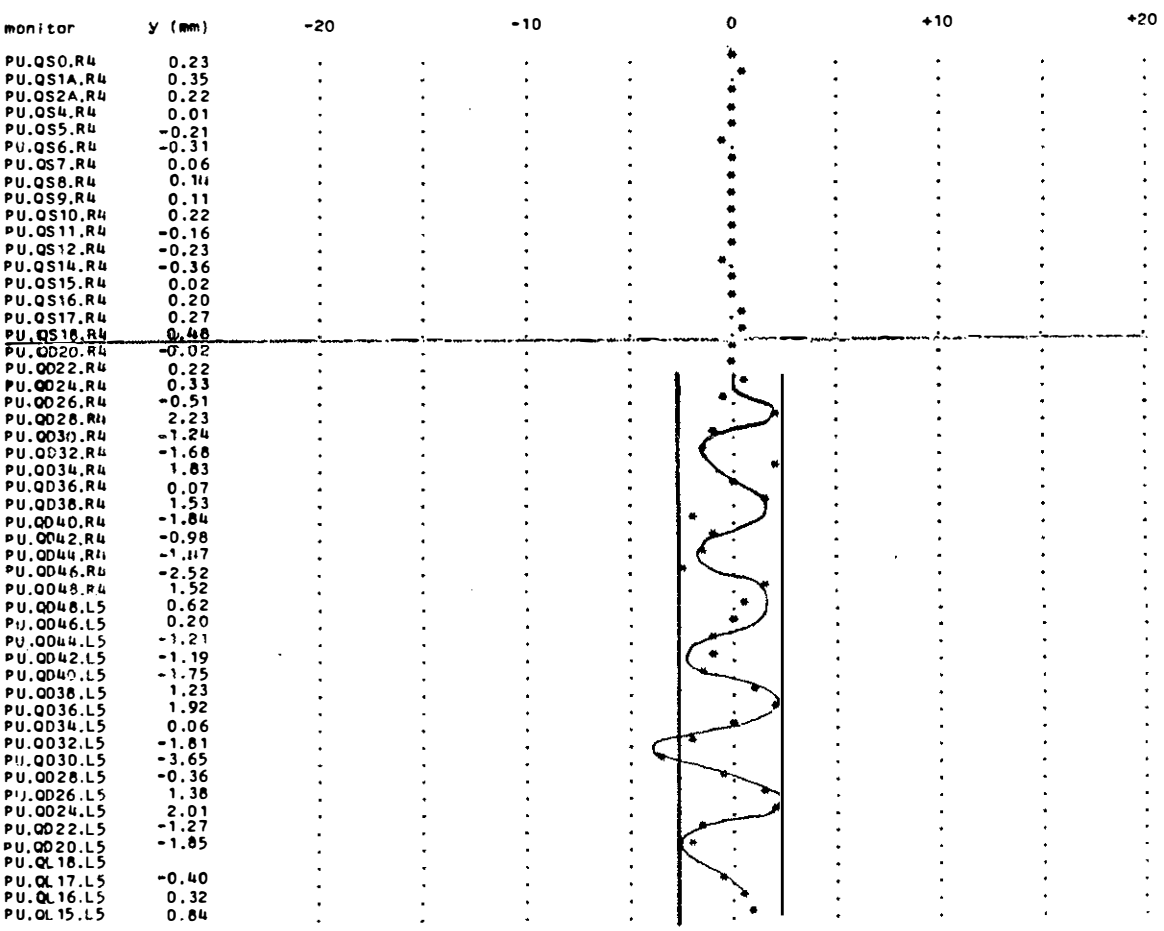

ARC 4-5
20 GeV

Figure 8

it 2 ** LEP ring - measured orbit + β
VERT plane

monitor	y (mm)
PU.QL18.R5	0.03
PU.QL28.R5	0.07
PU.QL4.R5	0.41
PU.QL5.R5	0.01
PU.QL6.R5	-0.25
PU.QL7.R5	0.14
PU.QL8.R5	-0.21
PU.QL9.R5	-0.07
PU.QL10.R5	0.46
PU.QL11.R5	-0.07
PU.QL12.R5	0.07
PU.QL14.R5	0.11
PU.QL15.R5	
PU.QL16.R5	0.54
PU.QL17.R5	0.27
PU.QL18.R5	-0.06
PU.QD20.R5	-1.87
PU.QD22.R5	1.26
PU.QD24.R5	0.94
PU.QD26.R5	1.33
PU.QD28.R5	1.23
PU.QD30.R5	-0.91
PU.QD32.R5	-1.54
PU.QD34.R5	
PU.QD36.R5	1.46
PU.QD38.R5	1.17
PU.QD40.R5	-1.66
PU.QD42.R5	-0.85
PU.QD44.R5	-1.80
PU.QD46.R5	-0.36
PU.QD48.R5	2.88
PU.QD48.L6	1.51
PU.QD46.L6	-0.40
PU.QD44.L6	-3.10
PU.QD42.L6	-1.26
PU.QD40.L6	1.61
PU.QD38.L6	3.71
PU.QD36.L6	3.99
PU.QD34.L6	-1.53
PU.QD32.L6	-4.27
PU.QD30.L6	-3.23
PU.QD28.L6	
PU.QD26.L6	4.70
PU.QD24.L6	3.04
PU.QD22.L6	-2.17
PU.QD20.L6	-5.09
PU.QS18.L6	-3.40
PU.QS17.L6	-0.59
PU.QS16.L6	1.41
PU.QS15.L6	
PU.QS14.L6	4.67
PU.QS12.L6	0.56

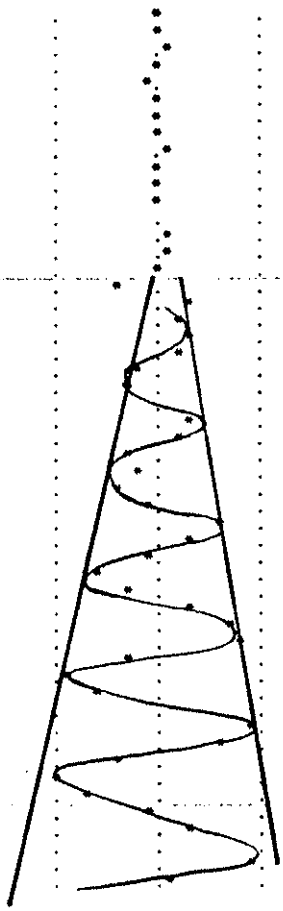

ARC 5-6
20 GeV

Figure 9

it 3 ** LEP ring - measured orbit + β oscillation
VERT plane

monitor	y (mm)
PU.QSD.R6	0.14
PU.QS1A.R6	0.13
PU.QS2A.R6	0.20
PU.QS4.R6	0.06
PU.QS5.R6	-0.49
PU.QS6.R6	0.30
PU.QS7.R6	-0.42
PU.QS8.R6	0.11
PU.QS9.R6	0.18
PU.QS10.R6	-0.02
PU.QS11.R6	0.07
PU.QS12.R6	-0.29
PU.QS14.R6	0.18
PU.QS15.R6	-0.05
PU.QS16.R6	0.79
PU.QS17.R6	
PU.QS18.R6	
PU.QD20.R6	-0.60
PU.QD22.R6	
PU.QD24.R6	0.62
PU.QD26.R6	0.04
PU.QD28.R6	0.13
PU.QD30.R6	0.16
PU.QD32.R6	-1.78
PU.QD34.R6	
PU.QD36.R6	1.35
PU.QD38.R6	0.95
PU.QD40.R6	-0.19
PU.QD42.R6	-2.73
PU.QD44.R6	-0.83
PU.QD46.R6	-0.54
PU.QD48.R6	1.16
PU.QD48.L7	2.69
PU.QD46.L7	-1.21
PU.QD44.L7	-2.30
PU.QD42.L7	-2.72
PU.QD40.L7	0.62
PU.QD38.L7	2.63
PU.QD36.L7	3.02
PU.QD34.L7	-3.00
PU.QD32.L7	-3.66
PU.QD30.L7	-2.10
PU.QD28.L7	2.55
PU.QD26.L7	5.08
PU.QD24.L7	0.18
PU.QD22.L7	-1.12
PU.QD20.L7	-4.97
PU.QL18.L7	-4.17
PU.QL17.L7	-0.29
PU.QL16.L7	1.43
PU.QL15.L7	2.18

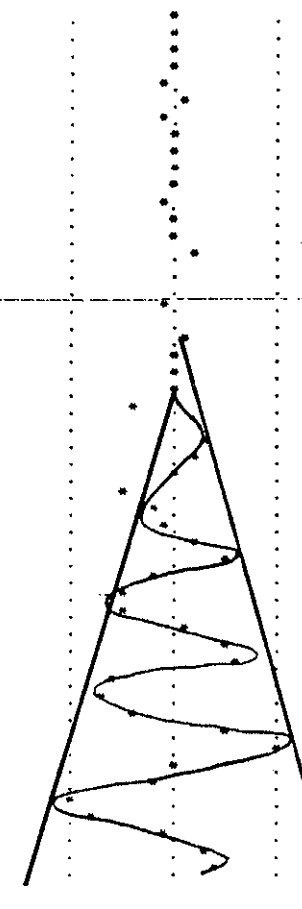

ARC 6-7
20 GeV

Figure 10

it 2 ** LEP ring - measured orbit $+\beta$
VERT plane

monitor	y (mm)
PU.QL1B.R7	0.01
PU.QL2B.R7	0.19
PU.QL4.R7	0.57
PU.QL5.R7	0.03
PU.QL6.R7	-0.04
PU.QL7.R7	0.11
PU.QL8.R7	-0.10
PU.QL9.R7	0.19
PU.QL10.R7	1.40
PU.QL11.R7	0.09
PU.QL12.R7	0.19
PU.QL14.R7	0.33
PU.QL15.R7	0.12
PU.QL16.R7	0.77
PU.QL17.R7	0.23
PU.QL18.R7	0.46
PU.QD20.R7	-0.99
PU.QD22.R7	3.23
PU.QD24.R7	
PU.QD26.R7	0.69
PU.QD28.R7	-0.20
PU.QD30.R7	-1.33
PU.QD32.R7	-2.06
PU.QD34.R7	5.29
PU.QD36.R7	1.99
PU.QD38.R7	-0.45
PU.QD40.R7	
PU.QD42.R7	-2.80
PU.QD44.R7	-2.25
PU.QD46.R7	-0.31
PU.QD48.R7	2.43
PU.QD48.L8	1.32
PU.QD46.L8	-0.23
PU.QD44.L8	-2.95
PU.QD42.L8	-3.20
PU.QD40.L8	1.24
PU.QD38.L8	4.23
PU.QD36.L8	4.02
PU.QD34.L8	1.37
PU.QD32.L8	-4.73
PU.QD30.L8	0.71
PU.QD28.L8	0.08
PU.QD26.L8	4.57
PU.QD24.L8	5.45
PU.QD22.L8	-2.21
PU.QD20.L8	-5.50
PU.QS18.L8	-4.33
PU.QS17.L8	-0.47
PU.QS16.L8	1.89
PU.QS15.L8	2.84
PU.QS14.L8	4.54
PU.QS12.L8	0.46

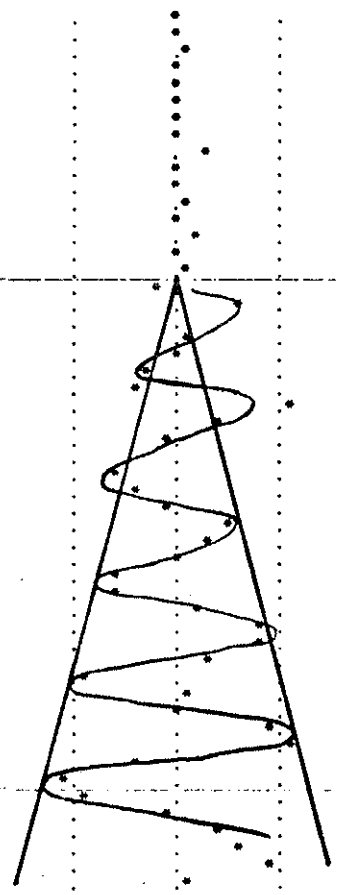

ARC 7-8
20 GeV

Figure 11

it 2 ** LEP ring - measured orbit $+\beta$
VERT plane

monitor	y (mm)
PU.QS0.R8	0.24
PU.QS1A.R8	0.31
PU.QS2A.R8	0.10
PU.QS4.R8	0.16
PU.QS5.R8	0.12
PU.QS6.R8	0.31
PU.QS7.R8	0.32
PU.QS8.R8	-0.14
PU.QS9.R8	-0.19
PU.QS10.R8	-0.15
PU.QS11.R8	-0.03
PU.QS12.R8	0.70
PU.QS14.R8	0.43
PU.QS15.R8	0.70
PU.QS16.R8	0.81
PU.QS17.R8	0.19
PU.QS18.R8	
PU.QD20.R8	0.87
PU.QD22.R8	1.69
PU.QD24.R8	-0.05
PU.QD26.R8	1.40
PU.QD28.R8	0.10
PU.QD30.R8	-1.36
PU.QD32.R8	-2.13
PU.QD34.R8	-0.54
PU.QD36.R8	1.24
PU.QD38.R8	1.50
PU.QD40.R8	-0.34
PU.QD42.R8	
PU.QD44.R8	
PU.QD46.R8	0.89
PU.QD48.R8	2.88
PU.QD48.L1	1.52
PU.QD46.L1	-1.33
PU.QD44.L1	-3.51
PU.QD42.L1	-4.26
PU.QD40.L1	3.74
PU.QD38.L1	4.38
PU.QD36.L1	2.76
PU.QD34.L1	-0.43
PU.QD32.L1	-5.14
PU.QD30.L1	-1.40
PU.QD28.L1	0.86
PU.QD26.L1	5.52
PU.QD24.L1	4.04
PU.QD22.L1	-1.83
PU.QD20.L1	-5.95
PU.QL18.L1	-4.79
PU.QL17.L1	-0.48
PU.QL16.L1	2.77
PU.QL15.L1	3.00
PU.QL14.L1	5.60

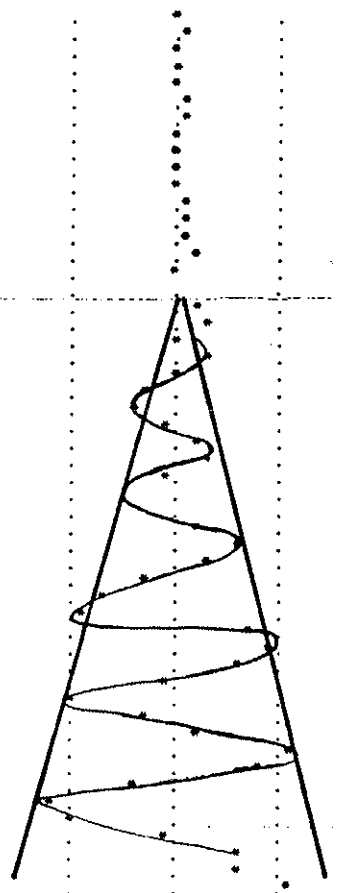

ARC 8-1
20 GeV

Figure 12

it 2 ** LEP ring - measured orbit + β oscillation
VERT plane

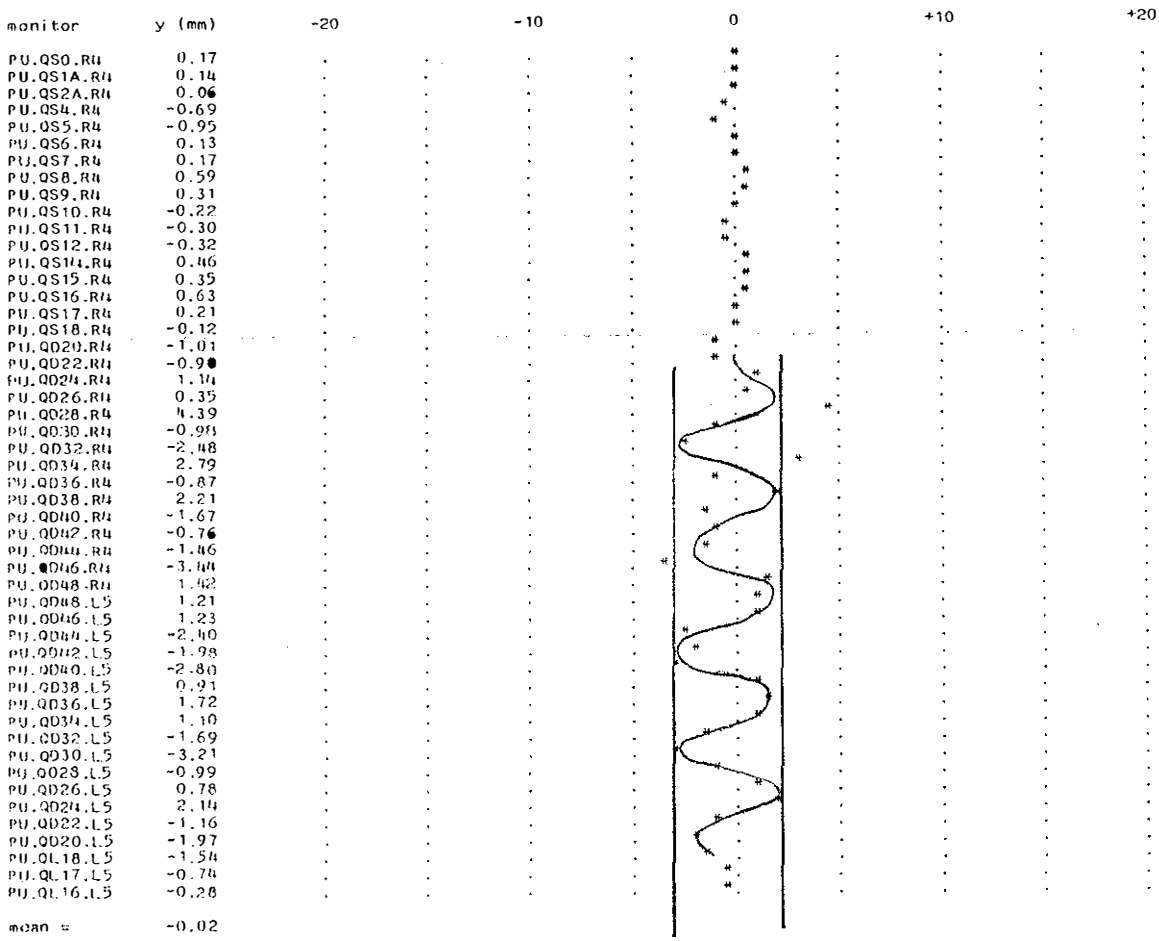

ARC 4-5
46 GeV

Figure 13